HHS Public Access

Author manuscript

Nat Nanotechnol. Author manuscript; available in PMC 2013 May 01.

Published in final edited form as:

Nat Nanotechnol. 2012 November ; 7(11): 733–736. doi:10.1038/nnano.2012.163.

Determination of the elastic moduli of thin samples and adherent cells using conical AFM tips

Núria Gavara[*,+] and **Richard S. Chadwick**[*]

[*]Auditory Mechanics Section, National Institute on Deafness and Other Communication Disorders, National Institutes of Health, Bethesda, MD 20892.

The atomic force microscope (AFM) can detect the mechanical fingerprints of normal and diseased cells at the single cell level under physiological conditions[1,2]. However, AFM studies of cell mechanics is limited by the "bottom effect" artifact that arises from the stiff substrates used to culture cells. Because cells adhered to substrates are very thin[3], this artifact makes cells appear stiffer than they really are[4]. Here we show an analytical correction that accounts for this artifact when conical tips are used for AFM measurements of thin samples. Our Bottom Effect Cone Correction (BECC) corrects the Sneddon's model[5], which is widely used to measure Young's modulus (*E*). Comparing the performance of BECC and Sneddon's model on thin polyacrylamide gels, we find that while Sneddon's model overestimates *E*, BECC yields *E* values that are thickness-independent and similar to those obtained on thick regions of the gel. Application of BECC to measurements on live adherent fibroblasts demonstrates a significant improvement on the estimation of their local mechanical properties.

The pioneering work of Lekka *et al.* showed that AFM could be used to identify malignant cancer cells by measuring their reduced Young's modulus[6]. Following this work, similar studies on different types of cancer cells have emerged[7–9], along with a better understanding of how various factors (such as the coating of the cell substrate, force loading rate or culture time) influence the ability to unequivoquely distinguish a malignant cell from a normal one[10,11]. Altered mechanical phenotypes have also been characterized using AFM for other pathological conditions and diseases (for a review see Kuznetsova *et al.*[12]).

It is widely acknowledged that AFM measurements on adherent cells are affected by artifacts stemming from the large stiffness of the substrates typically used for cell culture[3]. For that reason, AFM users limit the indentations to 10% of the cell's thickness[13].

Corresponding author: Richard S. Chadwick, Auditory Mechanics Section, NIDCD/NIH, Building 10, Room 5D/49, 10 Center Drive, MSC 1417, Bethesda, MD 20892, Phone: (301) 435-1957, Fax: (301) 480-1716, chadwick@helix.nih.gov.
[+]Present address: Drittes Physikaliches Institut, Georg-August-Universität, Göttingen, Germany.

Author contributions

N.G. conceived, designed and performed the experiments and analysed the data. R.S.C. developed the BECC correction. N.G. and R.S.C. co-wrote the paper.

Supplementary information

Supplementary information accompanies this paper at www.nature.com/naturenanotechnology. Reprints and permission information is available online at http://npg.nature.com/reprintsandpermissions/.

Nevertheless, >400 nm indentations are required to avoid errors due to uncertain determination of the contact point[14]. As a result, measurements are restricted to the central region of the cell[10,13], likely probing the mechanics of the nucleus rather than the cytoskeleton. A less restrictive approach would use a more sophisticated model that accounts for the bottom effect when estimating (*E*). We previously derived such a model for spherical tips[4]. Nevertheless, sharpened tips are better suited to reach the full potential of AFM as a high-resolution biomechanical tool, since they allow for simultaneous topographical and nanomechanical mapping of single cells[2,14].

To that account, we have now derived BECC, a multiplicative analytical correction to the commonly used Sneddon's Model (SM) for conical tips[5]:

$$F=\frac{8E\tan\theta\delta^2}{3\pi}\left\{1+1.7795\frac{2\tan\theta}{\pi^2}\frac{\delta}{h}+16(1.7795)^2\tan^2\theta\frac{\delta^2}{h^2}+\mathrm{O}\left(\frac{\delta^3}{h^3}\right)\right\}$$

where *F* is the applied force, δ is indentation, θ is the half-opening angle of the cone, *h* is the height of the sample at that location, and Poisson's ratio was assumed to be 0.5 (formula derivation can be found in online materials).

To compare the performance of BECC and SM, we used polyacrylamide gels of graded thickness (<1 μm to hundreds of microns), specifically crafted to resemble the height profile of an adherent cell (fig1C, suppl. fig1). Polyacrylamide gels are homogenous and isotropic, which makes them an ideal substrate to test Hertzian-like contact models like SM or BECC. We find that SM grossly overestimates *E* up to 100-fold, with values heavily dependent on gel thickness (Fig1A, Fig2A). Conversely, when we use BECC, computed values for *E* are thickness-independent (fig1B) and similar to the values obtained on thick regions of the same gel (suppl. Fig2A,C). Furthermore, BECC performs equally well for a wide range of gel stiffness (Fig2B). When we intentionally applied very large indentations (>85% of gel thickness), the observed *E* values began to increase, likely indicating that we had reached the non-linear elasticity regime of the gel (suppl. Fig. 3).

We also compared our correction to the finite element calculation of Kang *et al*, who considered the indentation of a finite thickness soft incompressible elastic layer bonded to a rigid substrate by a slightly blunted rigid frictionless cone[15]. When we input the parameters used in our experiments, our analytical result and the finite element result agree within 4% of each other (see online materials).

We then tested the performance of BECC on measurements carried out on adherent fibroblasts cultured on fibronectin-coated glass surfaces. To avoid remodelling of the cytoskeleton due to prolonged cell poking or too large applied forces, we limited our indentations to ~500 nm, using maximal forces of 2.5 nN and being in contact with the cell only for ~12% of the cycle time. As shown in fig 3, we were able to discern regions with distinct ranges of stiffness, likely corresponding to stress fibres or the nucleus (Fig. 3B). The location of those regions, as well as the height profile of the cell, was in agreement with the cell morphology observed in the phase contrast image that was recorded simultaneously

(Fig. 3C–D). On the contrary, regions of distinct stiffness were barely evident when using SM (Fig. 3A).

To characterize the mechanical cell phenotype associated with a disease, multiple locations (usually on thick regions) are probed for each cell, and several cells on a population are studied. For our cell type and culture conditions, we find that cell regions up to 4 μm thickness display the largest variability (Fig 4). Therefore, targeting measurements to these cell regions would maximize the odds of measuring a statistically significant difference in cell mechanical properties when studying a disease or pharmacological treatment. We thus recommend a similar preliminary assessment when performing AFM indentation measurements to distinguish mechanical cell phenotypes. Standard studies pool together *E* values obtained from many cells, usually displaying the data in the form of histograms[8]. It has been suggested that the skewness of the *E* distribution constitutes a reliable fingerprint of diseased cell populations[8]. Not surprisingly, we find that when the bottom effect is not corrected, the distribution of *E* values becomes artifactually skewed to the right (suppl. Fig. 3A), mainly due to the overestimated *E* values that thin areas contribute to the distribution. Thus, in light of our results, bottom effect artifacts should be ruled out to all certainty before using skewness as a mechanical hallmark of disease. Another artifact arising from the bottom effect impacts the determination of the contact point, which is slightly displaced to the right of the force-indentation curve when using SM (suppl. Fig. 4). As a result, thin regions appear to be even thinner. This artifact is again corrected using BECC and should be considered when performing force-volume measurements that correlate AFM mechanical measurements with cell topography[11,16].

Both SM and BECC are Hertzian-like models that attempt to characterize the whole mechanical response of an adherent cell with a single parameter *E*. A more complete approach would be to generate a completely new constitutive model that takes into account the true cell architecture, including the presence of a membrane, a heterogeneous cytoskeleton and a nucleus. Such a model would then contain multiple parameters for the distinctive mechanical responses of these three elements[17]. Nevertheless this goal has not been fully achieved yet. Hertzian-like contact models have been extensively used as an alternative, although they make certain assumptions on the nature of the probed sample. Namely, they assume the sample is isotropic, homogeneous and linear elastic. These assumptions, which are not necessarily fulfilled by adherent cells, constitute the main limitations of applicability of these models. As a result, BECC can't, on its own, account for cell viscoelasticity or changes in cell stiffness along its depth. Nevertheless, researchers have devised clever ways to modify AFM force-displacement protocols, so that Hertzian-like models can provide additional information on the cell's mechanical behaviour. Cell viscoelasticity has been addressed by superimposing small oscillations to a constant indentation and analysing the results as a complex elastic modulus[18]. A recent approach based on multi-harmonic analysis yields a much larger throughput, and allows mapping of the local properties of a cell by using the 0th, 1st and 2nd harmonic components of the Fourier spectrum of the AFM cantilevers interacting with a cell's surface[19]. Mechanical heterogeneity along the cell thickness has been characterized by comparing the relative *E* values obtained from shallow and deep indentations[20]. In addition, a similar approach can be

used to measure non-linear elasticity[21]. Most importantly, since all these approaches are based on SM, our multiplicative correction can be readily combined with any of these protocols. For a discussion of additional potential model extensions, the reader is addressed to the online supplementary material.

In conclusion, BECC enables non-artifactual nanomechanical mapping of the whole cell surface using AFM. The correction can also be readily combined with existing protocols for viscoelasticy, non-linear elasticity and depth-sensing analysis. We thus predict that the mechanical abnormalities so far measured in diseased cells will be further evident once larger parts of the cell cytoskeleton are non-artifactually probed, thus solidifying AFM as a diagnostic tool for malignancy.

Methods

Preparation of polyacrylamide gels

Polyacrylamide gels constitute an elastic and repeatable test material, with small point-to-point variations in stiffness[22] (coefficient of variation for E is ~30%). Polyacrylamide gels were prepared via photopolymerization initiated by Irgacure 2959 as described previously[23]. Different final concentrations of acrylamide and bis-acrylamide were diluted in water to obtain gels of a wide range of stiffness A drop of gel mixture was deposited on a chemically activated glass slide and the drop was left uncovered. Polymerization was achieved by exposure to UV light. After polymerization, gels remained firmly attached to the slide and displayed a hill-like shape. At their edges, gels displayed a smoothly increasing height profile, with the thinnest areas being less than 1 μm tall.

Cells

Cell measurements were performed in living fibroblasts, cell line NIH-3T3 (CCL-1658, ATCC). The culture medium consisted of hepes-buffered DMEM (Gibco) with 10% calf serum (SAFC Biosciences) and 1:100 Penicillin-Streptomycin (Sigma). Measurements were performed on glass-bottomed petri dishes coated with fibronectin, at 37 °C by heating the stage of the microscope.

AFM setup

Measurements were performed using a Catalyst AFM (Bruker Corp.) instrument mounted on the stage of an Axiovert 200 inverted microscope (Zeiss) placed on a vibration-isolation table (Isostation). A V-shaped gold-coated silicon nitride cantilever with a four-sided pyramidal tip (MLCT, Bruker Corp.) was used as probe. The spring constant of the cantilever was 0.047± 0.003 N m^{-1} as calibrated using the thermal fluctuations method[24]. Detailed descriptions of the measurement protocol and data analysis can be found in the online methods.

Supplementary Material

Refer to Web version on PubMed Central for supplementary material.

Acknowledgements

We thank R. Sunyer, V. Luo and K.M. Yamada for critical input. This work was supported by the Intramural Program of the US National Institute of Deafness and Other Communication Disorders.

References

1. Lee GYH, Lim CT. Biomechanics approaches to studying human diseases. Trends Biotechnol. 2007; 25:111–118. [PubMed: 17257698]
2. Costa KD. Single-cell elastography: Probing for disease with the atomic force microscope. Dis. Markers. 2003–2004; 19:139–154. [PubMed: 15096710]
3. Lekka M, Laidler P. Applicability of AFM in cancer detection. Nature Nanotech. 2009; 4:72.
4. Dimitriadis EK, Horkay F, Maresca J, Kachar B, Chadwick R. Determination of Elastic Moduli of Thin Layers of Soft Material Using the Atomic Force Microscope. Biophys. J. 2002; 82:2798–2810. [PubMed: 11964265]
5. Sneddon, IN. Fourier Transforms. New York: McGraw-Hill; 1951. Ch. 10.
6. Lekka M, et al. Elasticity of normal and cancerous human bladder cells studied by scanning force microscopy. Eur. Biophys. J. 1999; 28:312–316. [PubMed: 10394623]
7. Cross SE, Jin Y-S, Rao JY, Gimzewski JK. Nanomechanical analysis of cells from cancer patients. Nature Nanotech. 2007; 2:780–783.
8. Cross SE, et al. AFM-based analysis of human metastatic cancer cells. Nanotech. 2008; 19:384003–384011.
9. Li QS, Lee GY, Ong CN, Lim CT. AFM indentation study of breast cancer cells. Biochem. Biophys. Res. Commun. 2008; 374:609–613. [PubMed: 18656442]
10. Lekka, et al. Cancer cell recognition – Mechanical phenotype. Micron. 2012 In press.
11. Prabhune M, et al. Comparison of mechanical properties of normal and malignant thyroid cells. Micron. 2012 In press.
12. Kuznetsova TG, et al. Atomic force microscopy probing of cell elasticity. Micron. 2007; 38:824–833. [PubMed: 17709250]
13. Cross SE, Jin Y-S, Rao J, Gimzewski JK. Applicability of AFM in cancer detection. Nature Nanotech. 2009; 4:72–73.
14. Rico F, et al. Probing mechanical properties of living cells by atomic force microscopy with blunted pyramidal cantilever tips. Phys. Rev. E. 2005; 72:021914.
15. Kang I, et al. Changes in the Hyperelastic Properties of Endothelial Cells Induced by Tumor Necrosis Factor-α. Biophys. J. 2008; 94:3273–3285. [PubMed: 18199670]
16. Kihara T, Haghparast SMA, Shimizu Y, Yuba S, Miyake J. Physical properties of mesenchymal stem cells are coordinated by the perinuclear actin cap. Biochem. Bioph. Res. Co. 2011; 409:1–6.
17. McElfresh M, et al. Combining constitutive materials modeling with atomic force microscopy to understand the mechanical properties of living cells. Proc. Natl. Acad. Sci. U.S.A. 2002; 99(Suppl 2):6493–6497. [PubMed: 11983924]
18. Alcaraz J, et al. Microrheology of Human Lung Epithelial Cells Measured by Atomic Force Microscopy. Biophys. J. 2003; 84:2071–2079. [PubMed: 12609908]
19. Raman A, et al. Mapping nanomechanical properties of live cells using multi-harmonic atomic force microscopy. Nature Nanotech. 2011; 6:809–814.
20. Pogoda K, et al. Depth-sensing analysis of cytoskeleton organization based on AFM data. Eur. Biophys. J. 2012; 41:79–87. [PubMed: 22038077]
21. Petrie RJ, Gavara N, Chadwick RS, Yamada KM. Nonpolarized signaling reveals two distinct modes of 3D cell migration. J. Cell Biol. 2012; 197:439–455. [PubMed: 22547408]
22. Gavara N, Chadwick RS. Noncontact microrheology at acoustic frequencies using frequency-modulated atomic force microscopy. Nat. Methods. 2010; 7:650–654. [PubMed: 20562866]
23. Wong JY, Velasco A, Rajagopalan P, Pham Q. Directed Movement of Vascular Smooth Muscle Cells on Gradient-Compliant Hydrogels. Langmuir. 2003; 19:1908–1913.

24. Butt HJ, Jaschke M. Calculation of thermal noise in atomic force microscopy. Nanotechnology. 1995; 6:1–7.

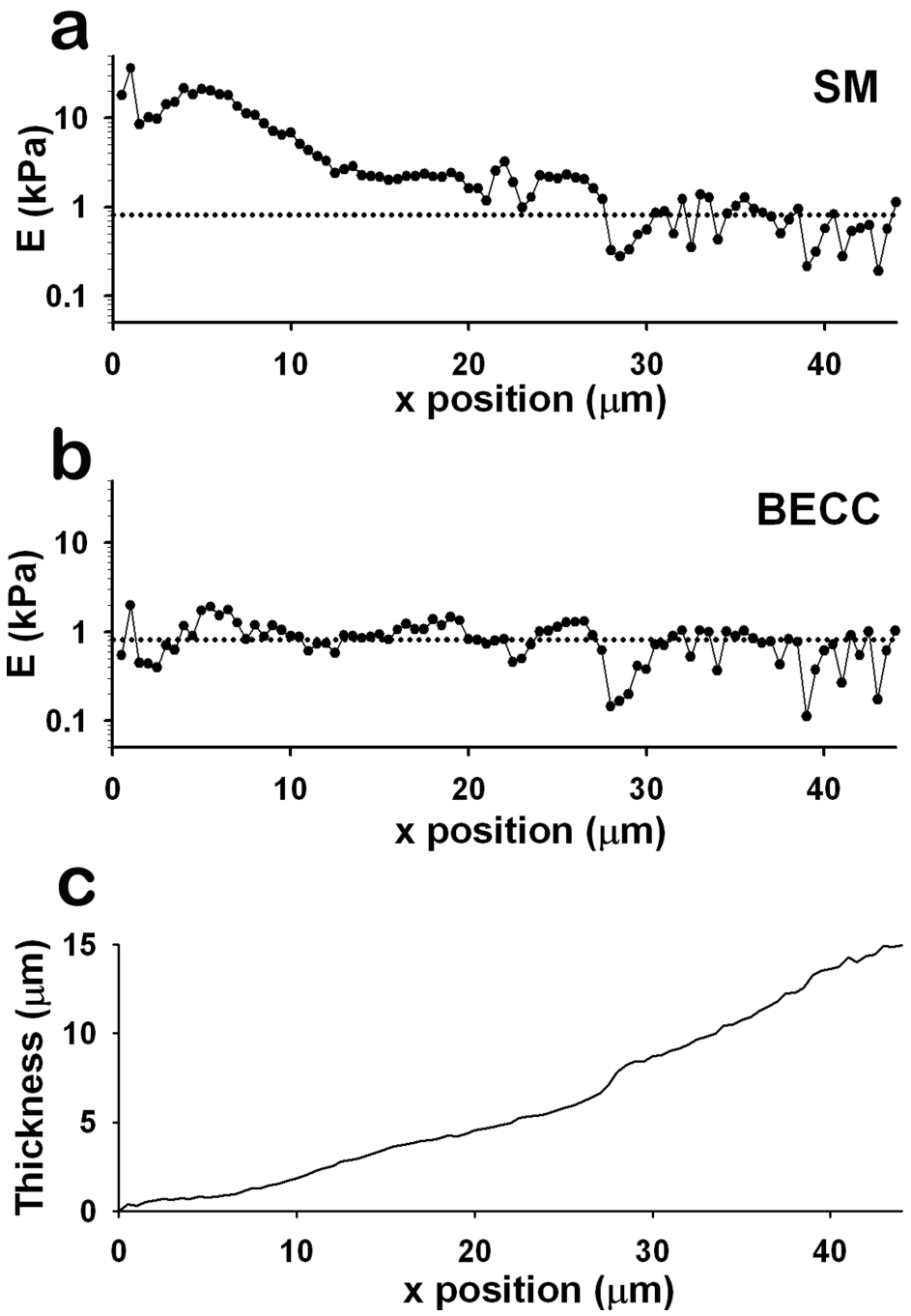

Figure 1.

BECC removes the bottom-effect artifact in measurements performed on thin gel samples. Young's modulus obtained from a line scan of a 0.8 kPa gel edge, computed using SM (***a***) or BECC (***b***), and thickness profile (***c***). Dotted line corresponds to E_{gel}, the average of all E values computed using BECC for multiple line scans of the same gel.

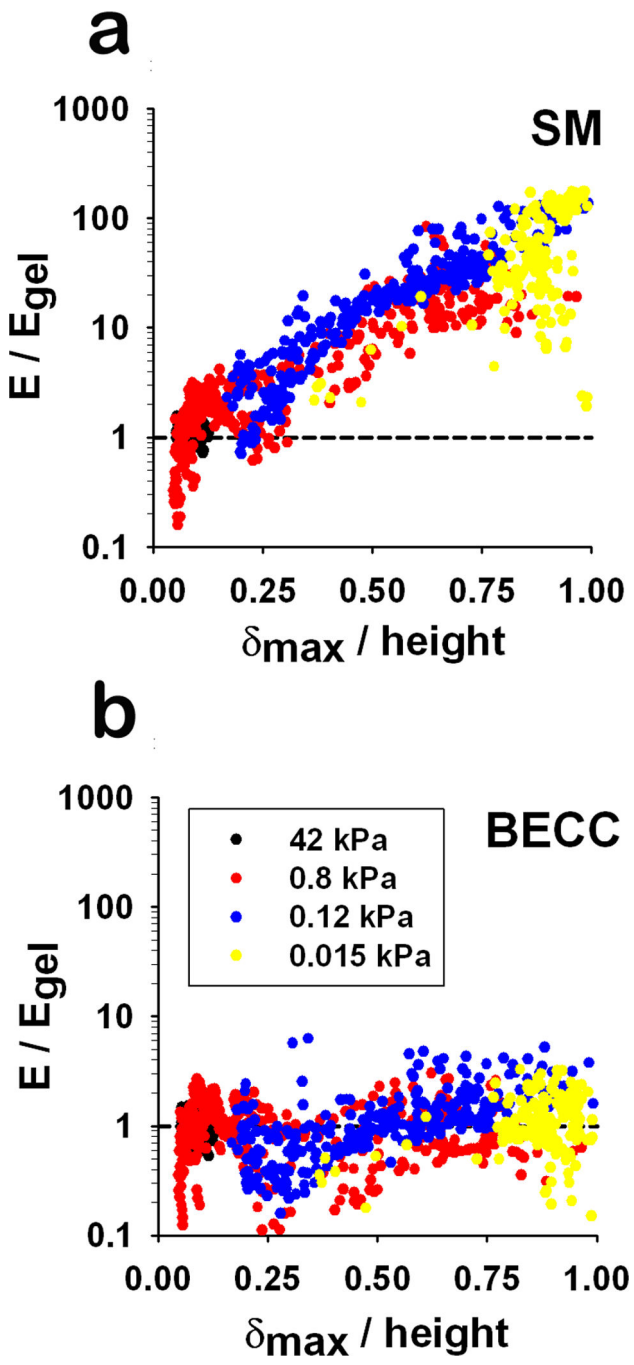

Figure 2.

Indentations larger than 10% of sample thickness result in very large overestimaton of the elastic modulus. Dependence of *E* values on the ratio between maximum indentation and gel thickness when using SM (***a***) or BECC (***b***). All data points are normalized by E_{gel} corresponding to the gel stiffness as indicated by the color code.

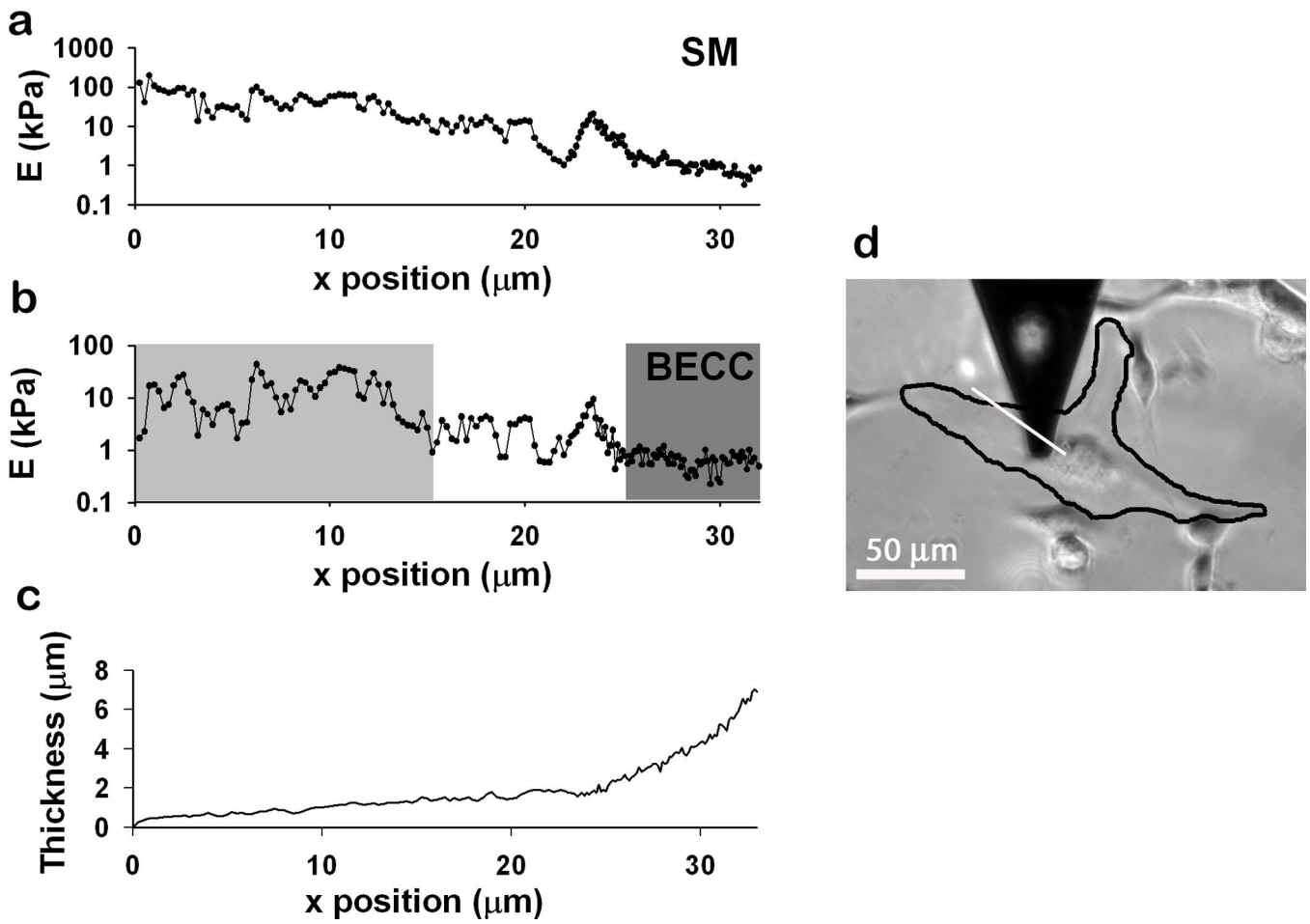

Figure 3.

BECC allows non-artifactual measurement of the local elastic moduli of adherent cells. Young's modulus obtained from a living NIH3T3 cell, computed using SM (***a***) or BECC (***b***) and thickness profile (***c***). Light grey shading indicates a region likely to be rich in stress fibres, whereas dark grey shading indicates the nucleus. The approximate direction of the line scan is superimposed as a white line on the phase contrast image of the outlined cell (***d***). Scale bar is 50 μm.

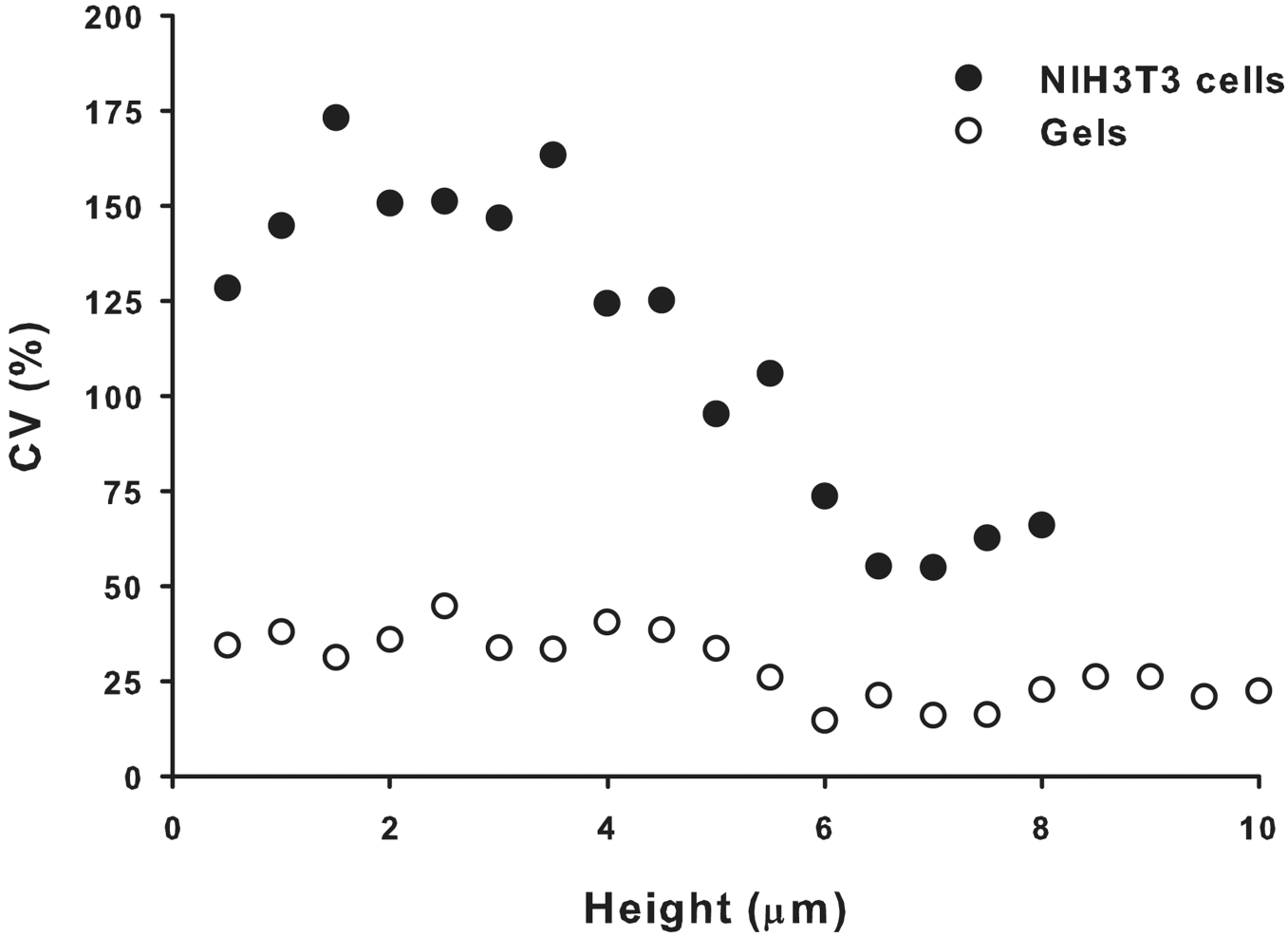

Figure 4.

NIH3T3 cells display largest *E* variability on regions <4 μm thick. Filled symbols correspond to the coefficient of variation (*CV*) of *E* values obtained on cells (*n*=50), whereas open symbols correspond to *CV* of *E* values obtained on gels (*n*=9). A minimum of 10 *E* values were pooled together to compute each data point in the graph.